Cooperative Received Signal Strength-Based Sensor Localization with Unknown Transmit Powers

Reza Monir Vaghefi, *Student Member, IEEE,* Mohammad Reza Gholami, *Student Member, IEEE,*
R. Michael Buehrer, *Senior Member, IEEE,* and Erik G. Ström, *Senior Member, IEEE,*

Abstract

Cooperative localization (also known as sensor network localization) using received signal strength (RSS) measurements when the source transmit powers are different and unknown is investigated. Previous studies were based on the assumption that the transmit powers of source nodes are the same and perfectly known which is not practical. In this paper, the source transmit powers are considered as nuisance parameters and estimated along with the source locations. The corresponding Cramér-Rao lower bound (CRLB) of the problem is derived. To find the maximum likelihood (ML) estimator, it is necessary to solve a nonlinear and nonconvex optimization problem, which is computationally complex. To avoid the difficulty in solving the ML estimator, we derive a novel semidefinite programming (SDP) relaxation technique by converting the ML minimization problem into a convex problem which can be solved efficiently. The algorithm requires only an estimate of the path loss exponent (PLE). We initially assume that perfect knowledge of the PLE is available, but we then examine the effect of imperfect knowledge of the PLE on the proposed SDP algorithm. The complexity analyses of the proposed algorithms are also studied in detail. Computer simulations showing the remarkable performance of the proposed SDP algorithm are presented.

R. M. Vaghefi and R. M. Buehrer are with the Mobile and Portable Radio Research Group, Bradley Department of Electrical and Computer Engineering, Virginia Polytechnic Institute and State University (Virginia Tech), Blacksburg, VA 24061 USA (e-mail: vaghefi@vt.edu; buehrer@vt.edu)

M. R. Gholami and E. G. Ström are with the Division of Communication Systems and Information Theory, Department of Signals and Systems, Chalmers University of Technology, SE-412 96 Gothenburg, Sweden (e-mail: moreza@chalmers.se; erik.strom@chalmers.se).

This work was supported in part by the Swedish Research Council (contract no. 2007-6363). This paper was presented in part at the IEEE International Conference on Acoustics, Speech and Signal Processing (ICASSP), Prague, Czech Republic, May 22-27, 2011.

Index Terms

Received Signal Strength (RSS), cooperative sensor localization, transmit power, maximum likelihood (ML), semidefinite programming (SDP), linear least squares (LLS), path loss exponent (PLE), computational complexity.

I. Introduction

Recently, wireless sensor networks (WSN) have been the subject of great interest in many studies because of their wide applications in control, tracking, and monitoring. Location information is a vital aspect of many WSNs. Indeed, the location of each sensor is often required to make the collected information useful. Generally, in a WSN, the positions of a number of sensors are known (anchor nodes), while there are some sensors (source nodes) whose positions are unknown and thus must be estimated using sensor localization. The main purpose of sensor localization is to determine the location of sensors in a WSN via noisy measurements [1]. These measurements may include received signal strength (RSS) [2]–[4], time-of-arrival [5], [6], time-difference-of-arrival [7]–[9], and angle-of-arrival [10], [11]. Among the different types of measurements, RSS is a popular method mainly because of its low complexity and cost in software and hardware implementations [1].

Sensor localization is generally divided into two cases: non-cooperative and cooperative. In the non-cooperative case, source nodes can communicate only with anchor nodes [1], [12]. The lack of accessible anchor nodes and also limited connectivity among anchor nodes and source nodes have led to the emergence of cooperative localization in which source nodes are able to communicate with both anchor nodes and other source nodes. Therefore, not only are the RSS values between source nodes and anchor nodes (source-anchor measurements) measured, but also the source nodes themselves are involved and collect RSS measurements from each other (source-source measurements). Furthermore, in cooperative localization, anchor nodes can estimate the location of all source nodes simultaneously. Thus, both estimation performance and robustness are improved by employing cooperative localization [1], [3], [13].

The maximum likelihood (ML) estimator and the Cramér-Rao lower bound (CRLB) of cooperative RSS localization were studied in [1]. The cost function of the ML estimator is severely nonlinear and noncovex and, therefore, it can be optimized by iterative algorithms only with an appropriate initialization [14], [15].

The performance of iterative algorithms strongly depends on the initial solution. If the initialization is not sufficiently close to the global minimum, the iterative algorithm may converge to a local minimum or a saddle point causing a large estimation error. Therefore, determining an appropriate initialization point is a crucial problem in optimizing the ML cost function. As a result, some approaches such as grid search methods, linear estimators, and convex relaxation techniques have been introduced to address the ML problem [3], [12], [16]. The grid search methods are not generally popular because they are very time-consuming and require a huge amount of memory when the number of the unknown parameters is too large. Linear estimators having a closed-form solution are usually derived based on many approximations [12], [17]–[19] which affect its performance, especially when shadowing is very high [19]. A convex relaxation technique such as semidefinite programming (SDP) is another solution for the ML convergence problem [13], [16], [19]–[24]. In the semidefinite relaxation technique, the nonlinear and nonconvex ML problem is transformed into a convex optimization problem. The advantage of an SDP is that its cost function does not have local minima and thus convergence to the global minimum is guaranteed [25], [26]. The downside is that the SDP technique is sub-optimal and cannot achieve the best possible performance in all conditions. Most studies mentioned above on RSS localization assume that the source transmit powers are the same and known [4], [13], [17], [23].

The RSS measurement model depends on the transmit power of the source nodes. Therefore, the anchor nodes are not able to find the location of a source node if its transmit power is not accounted for. Each source node has a specific transmit power depending on, e.g., its battery and antenna gain. In addition, the transmit power might change with time, e.g., when batteries begin to exhaust. Consequently, each source node has to report its transmit power to anchor nodes constantly during RSS measurements which requires additional hardware and software in both anchor nodes and source nodes making the network more convoluted [1]. When the transmit powers are not available, there are generally two common solutions suggested to address this problem. First, one can estimate the transmit power of the source along with its location [19], [27]. Second, one can eliminate the dependency of the transmit power from the RSS measurement model by using the differential RSS between a source node and two anchor nodes [19], [28], [29]. The number of unknown parameters in the latter method is fewer than in the former method. However, employing the latter method introduces noise correlation and noise enhancement which complicate the computations and degrade the accuracy [19]. It should also be noted that all previous

studies on RSS localization with unknown transmit power are for the non-cooperative case. In this paper, for the first time, we examine this problem for the cooperative localization case. Some range-free and non-model-based techniques were also suggested [30], [31] in which the localization algorithms do not require the model parameters, such as the transmit power and the path loss exponent, and the estimate of the source location was basically obtained based on the comparisons among RSS measurements. However, having a cooperative network and source nodes with different transmit powers make those algorithms complex and inapplicable.

Thus, cooperative localization using RSS in the practical case where transmit powers are different and unknown is currently an open problem. In this paper, we consider this problem and provide a solution. Specifically, the source transmit powers are considered as nuisance parameters and estimated jointly with the source node locations. A novel SDP technique is introduced for this expanded estimation problem. To make the derivations easier to understand, we start by describing the proposed SDP algorithm for the non-cooperative case. Then, the measurement model is extended to the cooperative case and the corresponding SDP algorithm is derived. The original ML estimator is transformed into an approximate nonlinear least squares (NLS) problem. Then, an appropriate relaxation is applied to convert the NLS problem into an SDP optimization problem. It is worth mentioning that the SDP techniques introduced in [16], [20] are not applicable here, since they assumed that noisy pairwise distances between source nodes and anchor nodes are available. However, in our study, the distances cannot be computed because the transmit powers of the source nodes are not available to the estimator. Ouyang et al. [13] also derived an SDP approach which is directly applied to the RSS model. However, they assumed that all source nodes have the same known transmit power which is not practical. Conversely, in the current work, we assume that each source node has a unique transmit power which is not known. The Cramér-Rao lower bound (CRLB) of this problem is computed. We also propose a linear estimator for comparison with the proposed SDP algorithm. Moreover, we investigate the effect of imperfect knowledge of the path loss exponent (PLE) on the algorithms' accuracy and introduce a novel technique to improve performance when the PLE is estimated. We also study the computational complexity of the considered algorithms in detail.

The rest of the paper is organized as follows. Section II presents the non-cooperative RSS localization problem, introducing the measurement model and proposed localization algorithms. The extension of RSS

localization to the cooperative case is discussed in Section III. Section IV describes the effect of imperfect knowledge of the PLE on the proposed algorithms. Complexity analyses of the proposed algorithms are given in Section V. The simulation results and algorithm comparisons are discussed in Section VI. Finally, Section VII concludes the paper. In Appendix A, the corresponding CRLB of the measurement model is derived. The proposed linear estimator is derived in Appendix B. The full details of the complexity analyses are given in Appendix C.

Notation. Throughout the paper, the following notations are used. Lowercase and uppercase symbols denote scalar values. Bold uppercase symbols and bold lowercase symbols denote matrices and vectors, respectively. $\|\cdot\|$ denotes ℓ_2 norm. $\mathrm{diag}\{\cdot\}$ represents a diagonal matrix. $|\mathcal{A}|$ represents the cardinality (number of elements) of the set $\mathcal{A}$. $\mathbf{I}_M$ and $\mathbf{0}_M$ denote the M by M identity and the M by M zero matrices, respectively. For arbitrary symmetric matrices $\mathbf{A}$ and $\mathbf{B}$, $\mathbf{A} \succeq \mathbf{B}$ means that $\mathbf{A}-\mathbf{B}$ is positive semidefinite. $[\mathbf{a}]_i$ and $[\mathbf{A}]_{i,j}$ denote the ith element of vector $\mathbf{a}$ and the element at the ith row and jth column of matrix $\mathbf{A}$, respectively. $[\mathbf{A};\mathbf{B}]$ means that matrices $\mathbf{A}$ and $\mathbf{B}$ are concatenated vertically.

II. Non-cooperative Localization

This section describes the RSS localization model for the non-cooperative case. In non-cooperative localization problems, only the measurements between a source node and the anchor nodes are considered and the location of each source node is estimated independently. A network in a two-dimensional space is considered[1]. Let $\mathbf{x} = [a, b]^T \in \mathbb{R}^2$ be the unknown coordinates of the source node to be determined. Denote by $\mathcal{C} = \{1, \ldots, M\}$ the set of indices of the anchor nodes, by $\mathbf{y}_i = [x_i, y_i]^T \in \mathbb{R}^2$, $i \in \mathcal{C}$, the known location of the anchor nodes. Let $\mathcal{A} = \{\ i \mid i \in \mathcal{C}, \text{anchor node } i \text{ is connected to source node } \}$ be the set of the indices of the anchor nodes connected to the source node. The received power (in dBm) at the ith anchor node, P_i, under log-normal shadowing is modeled as [2]

$$P_i = P_0 - 10\beta \log_{10} \frac{d_i}{d_0} + n_i, \quad i \in \mathcal{A}, \tag{1}$$

where P_0 (in dBm) is the reference power at distance d_0 from the source (which depends on the transmit power), β is the path loss exponent, $d_i = \|\mathbf{y}_i - \mathbf{x}\|$ is the true distance between the source node and the ith anchor node, and n_i are the log-normal shadowing terms modeled as independent and identically

[1]The generalization to a three-dimensional space is straightforward, but is not explored in this paper.

distributed (i.i.d.) zero-mean Gaussian random variables with standard deviation σ_{dB} for $i \in \mathcal{A}$. The variance of the shadowing term is constant with distance and only depends on the environment where the network is set up [1]. Without loss of generality, we assume $d_0 = 1$ m. In this case, there are 3 unknown parameters that should be estimated including the source node coordinates and its transmit power.

A. Maximum Likelihood Estimator

The ML estimator is asymptotically efficient meaning that it can achieve the CRLB accuracy when the number of measurements tends to infinity [32, Ch. 7]. The ML estimator of the measurement model in (1) is obtained by the following nonconvex optimization problem [2], [19]

$$\hat{\boldsymbol{\theta}} = \underset{\boldsymbol{\theta}\in\mathbb{R}^3}{\arg\min} \sum_{i\in\mathcal{A}} \left(P_i - P_0 + 10\beta \log_{10} d_i\right)^2, \tag{2}$$

where $\boldsymbol{\theta} = [\mathbf{x}; P_0]$. We can write (2) equivalently as

$$\hat{\boldsymbol{\theta}} = \underset{\boldsymbol{\theta}\in\mathbb{R}^3}{\arg\min} \sum_{i\in\mathcal{A}} \left(\log_{10} \frac{h_i \lambda_i}{\alpha}\right)^2, \tag{3}$$

where $h_i \triangleq d_i^2$, $\lambda_i \triangleq 10^{P_i/5\beta}$, and $\alpha \triangleq 10^{P_0/5\beta}$. As mentioned before, a closed-form solution of (2) is not available and it should be approximately solved by numerical techniques [14], [32], [33]. The difficulty in finding the solution of the ML estimator leads us to employ suboptimal estimators, such as SDP and linear least squares (LLS) algorithms. The proposed SDP algorithm is derived in the next section. A linear estimator for the non-cooperative localization case was previously derived in [19].

B. Semidefinite Programming

This section describes the procedure of converting the ML problem of (2) into an SDP optimization problem. By rearranging the logarithmic term and dividing both sides by 5β, (1) can be reformulated as

$$\log_{10} d_i^2 \lambda_i = \frac{P_0}{5\beta} + \frac{n_i}{5\beta}. \tag{4}$$

Taking the power of 10 on both sides yields

$$d_i^2 \lambda_i = \alpha 10^{n_i/5\beta}. \tag{5}$$

For sufficiently small noise, the right-hand side (RHS) of (5) can be approximated using the first-order Taylor series expansion as

$$d_i^2 \lambda_i = \alpha \left(1 + \frac{\ln 10}{5\beta} n_i \right). \tag{6}$$

This can be rewritten as

$$d_i^2 \lambda_i = \alpha + \epsilon_i, \tag{7}$$

where ϵ_i is a zero-mean Gaussian random variable with variance $(\ln 10)^2 \alpha^2 \sigma_{dB}^2 / 25\beta^2$. The corresponding NLS estimator of the unknown parameters $[\hat{\mathbf{x}}; \hat{\alpha}]$ in (7) is [32, Ch. 8]

$$[\hat{\mathbf{x}}; \hat{\alpha}] = \underset{[\mathbf{x};\alpha] \in \mathbb{R}^3}{\arg\min} \sum_{i \in \mathcal{A}} \left(h_i \lambda_i - \alpha \right)^2. \tag{8}$$

The cost function (8) is still nonlinear and noncovex. In the next step, an auxiliary variable z is defined as

$$z = \mathbf{x}^T \mathbf{x}. \tag{9}$$

The minimization problem of (8) can be relaxed to an SDP optimization problem as [25]

$$\underset{\mathbf{x}, z, \alpha, h_i}{\text{minimize}} \quad \sum_{i \in \mathcal{A}} \left(h_i \lambda_i - \alpha \right)^2 \tag{10a}$$

$$\text{subject to } h_i = \begin{bmatrix} \mathbf{y}_i \\ -1 \end{bmatrix}^T \begin{bmatrix} \mathbf{I}_2 & \mathbf{x} \\ \mathbf{x}^T & z \end{bmatrix} \begin{bmatrix} \mathbf{y}_i \\ -1 \end{bmatrix}, \tag{10b}$$

$$\begin{bmatrix} \mathbf{I}_2 & \mathbf{x} \\ \mathbf{x}^T & z \end{bmatrix} \succeq \mathbf{0}_3. \tag{10c}$$

The solution of (10) can be effectively found with well known algorithms such as interior point methods [25], [26]. In MATLAB simulations, standard SDP solvers such as SeDuMi or SDPT3 [34], [35] are employed to solve SDP optimization problems. Note that we have employed the inequality constraint (10c) instead of the equality in (9) to relax the cost function in (8) to a convex problem in (10) [16], [20], [25].

In summary, an SDP solution for RSS localization with unknown transmit power is introduced by converting the nonconvex cost function of the ML estimator into a convex cost function using two steps of approximations and relaxations. In the first step, the ML cost function in (3) is approximated by

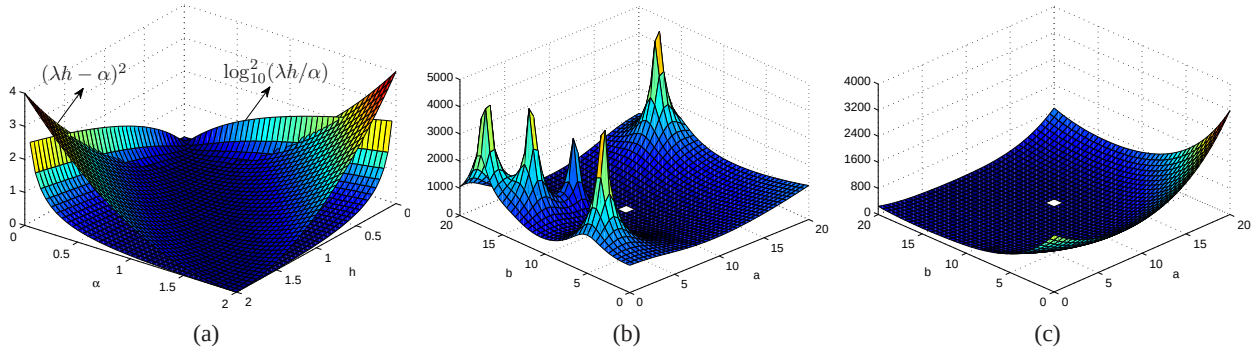

Fig. 1. (a) illustration of functions $(\lambda h-\alpha)^2$ and $\log_{10}^2(\lambda h/\alpha)$ versus unknown variables h and α (for simplicity, $\lambda=1$), (b) cost function of (3), (c) cost function of (8) versus a and b coordinates (source location), the minimum of the cost functions is indicated by a white square.

another cost function of (8). More specifically, the function $\sum_i(\lambda_i h_i-\alpha)^2$ is substituted for the function $\sum_i \log_{10}^2(\lambda_i h_i/\alpha)$. Fig. 1 depicts the two mentioned functions versus unknown parameters h and α (λ is a known parameter). As can be seen, these functions have similar behaviors; the minimum of both functions appears at $\lambda h=\alpha$ and both monotonically increase and decrease in the same regions. Note that the value λ changes the minimum of the functions but does not affect their general behaviors. Hence, for simplicity $\lambda=1$ has been selected for the illustration. Fig. 1 also depicts one realization of the ML cost function of (3) and the cost function of (8). A source is located at $[10,10]^T$ and five anchor nodes are randomly placed inside a square area 20 m $\times$ 20 m. The standard deviation of log-normal shadowing is 3 dB and the path loss exponent is set to 4. Since it is not possible to show a plot in four-dimensional space, the value of P_0 is fixed at the true value (-10 dBm) and the functions are plotted versus a and b coordinates. Fig. 1b shows the cost function of the ML estimator given in (3) which has a global minimum at $[10.5,11.5]^T$ (the step of the mesh grid is 0.5) and some local minima and saddle points, e.g., a local minimum at $[2.5,17.5]^T$. The cost function of (8), shown in Fig. 1c, is much smoother than (3) and has a global minimum at $[10,11.5]^T$. However, it has some concave areas around its global minimum. It, therefore, still must be relaxed to a convex shape. In the next step, by using the relaxation of (10c), the function in (8) is relaxed to a convex function in (10). The solution of (8) and (10) for the source location will coincide if the minimum of (10) occurs for $\mathbf{x}$ and z such that $z=\mathbf{x}^T\mathbf{x}$.

III. Cooperative Localization

This section describes the cooperative RSS localization model in which there are more than two source nodes with unknown locations, and moreover, source nodes can communicate not only with anchor nodes but also with each other [1]. Indeed, the power of the transmitted signal of each source can be measured at both anchor nodes and other source nodes. Therefore, two sets of RSS measurements are available to the estimator: source-anchor and source-source measurements. Denote by $\mathcal{S} = \{1, \ldots, N\}$ the set of indices of the source nodes and by $\mathbf{x}_j = [a_j, b_j] \in \mathbb{R}^2$, $j \in \mathcal{S}$, the coordinates of the jth source location. Let $\mathcal{A}_j = \{\ i \mid i \in \mathcal{C}, \text{anchor node } i \text{ is connected to source node } j\ \}$ be the set of the indices of the anchor nodes connected to the jth source node and $\mathcal{B}_j = \{\ i \mid i \in \mathcal{S},\ i > j, \text{source node } i \text{ is connected to source node } j\ \}$ be the set of indices of the source nodes connected to the jth source node. The cooperative RSS measurement model is expressed as [2]

$$P_{ij} = P_{0j} - 10\beta \log_{10} d_{ij} + n_{ij}, \quad j \in \mathcal{S},\ i \in \mathcal{A}_j \cup \mathcal{B}_j, \tag{11}$$

where P_{0j} is the reference power at a reference distance (1 m) from the jth source (which depends on the transmit power). $d_{ij} = \|\mathbf{y}_i - \mathbf{x}_j\|, i \in \mathcal{A}_j$, and $d_{ij} = \|\mathbf{x}_i - \mathbf{x}_j\|, i \in \mathcal{B}_j$. In addition, n_{ij} are the log-normal shadowing terms which are modeled as i.i.d. zero-mean Gaussian random variables with standard deviation σ_{dB}. In this case, there are in total $2N + N$ unknown parameters that should be estimated including the source node coordinates and transmit powers.

A. Maximum Likelihood Estimator

The corresponding ML estimator of the measurement model in (11) is obtained by the following nonconvex optimization problem [32, Ch. 7]

$$\hat{\boldsymbol{\phi}} = \underset{\boldsymbol{\phi} \in \mathbb{R}^{3N}}{\arg\min} \sum_{j \in \mathcal{S}} \sum_{i \in \mathcal{A}_j \cup \mathcal{B}_j} (P_{ij} - P_{0j} + 10\beta \log_{10} d_{ij})^2, \tag{12}$$

where $\boldsymbol{\phi} = [\mathbf{x}^T, \mathbf{p}_0^T]^T$ is the vector of unknown parameters to be estimated including $\mathbf{x} = [\mathbf{x}_1^T, \mathbf{x}_2^T, \ldots, \mathbf{x}_N^T]^T$ and $\mathbf{p}_0 = [P_{01}, P_{02}, \ldots, P_{0N}]^T$. Similarly to the non-cooperative case, (12) can be written alternatively as

$$\hat{\boldsymbol{\phi}} = \underset{\boldsymbol{\phi} \in \mathbb{R}^{3N}}{\arg\min} \sum_{j \in \mathcal{S}} \sum_{i \in \mathcal{A}_j \cup \mathcal{B}_j} \left(\log_{10} \frac{h_{ij} \lambda_{ij}}{\alpha_j} \right)^2, \tag{13}$$

where $h_{ij} \triangleq d_{ij}^2$, $\lambda_{ij} \triangleq 10^{P_{ij}/5\beta}$, and $\alpha_j \triangleq 10^{P_{0j}/5\beta}$. The proposed SDP algorithm is derived in the next section. We also formulate the proposed LLS algorithm for cooperative localization in Appendix B.

B. Semidefinite Programming

The SDP relaxation of cooperative RSS localization follows the same procedure as described previously for the non-cooperative case but with a slightly different relaxation. Consider similar approximations as applied to (4)-(8). Then, the ML cost function in (13) can be expressed approximately as [19]

$$[\hat{\mathbf{x}}; \hat{\boldsymbol{\alpha}}] = \underset{[\mathbf{x};\boldsymbol{\alpha}]\in\mathbb{R}^{3N}}{\arg\min} \sum_{j\in\mathcal{S}} \sum_{i\in\mathcal{A}_j\cup\mathcal{B}_j} \left(\lambda_{ij} h_{ij} - \alpha_j\right)^2, \tag{14}$$

where $\boldsymbol{\alpha} = [\alpha_1, \ldots, \alpha_N]^T$. Similarly to the non-cooperative case, the cost function of (14) is relaxed to a convex optimization problem. Let $\mathbf{X} = [\mathbf{x}_1, \mathbf{x}_2, \ldots, \mathbf{x}_N] \in \mathbb{R}^{2\times N}$ be the matrix of the source node coordinates. The auxiliary matrix $\mathbf{Z} \in \mathbb{R}^{N\times N}$ is introduced as

$$\mathbf{Z} = \mathbf{X}^T\mathbf{X}, \tag{15}$$

where $[\mathbf{Z}]_{ij} = \mathbf{x}_i^T\mathbf{x}_j$ is the (i,j)th element of the matrix $\mathbf{Z}$. The cost function (14) can be relaxed to an SDP optimization problem as [25]

$$\begin{aligned}
\underset{\mathbf{X},\mathbf{Z},\alpha_j,h_{ij}}{\text{minimize}} \quad & \sum_{j\in\mathcal{S}} \sum_{i\in\mathcal{A}_j\cup\mathcal{B}_j} \left(\lambda_{ij} h_{ij} - \alpha_j\right)^2 \\
\text{subject to} \quad & h_{ij} = \begin{bmatrix} \mathbf{y}_i \\ -\mathbf{e}_j \end{bmatrix}^T \begin{bmatrix} \mathbf{I}_2 & \mathbf{X} \\ \mathbf{X}^T & \mathbf{Z} \end{bmatrix} \begin{bmatrix} \mathbf{y}_i \\ -\mathbf{e}_j \end{bmatrix}, \ i \in \mathcal{A}_j, \\
& h_{ij} = \begin{bmatrix} \mathbf{0}_2 \\ \mathbf{e}_i - \mathbf{e}_j \end{bmatrix}^T \begin{bmatrix} \mathbf{I}_2 & \mathbf{X} \\ \mathbf{X}^T & \mathbf{Z} \end{bmatrix} \begin{bmatrix} \mathbf{0}_2 \\ \mathbf{e}_i - \mathbf{e}_j \end{bmatrix}, \ i \in \mathcal{B}_j, \\
& \begin{bmatrix} \mathbf{I}_2 & \mathbf{X} \\ \mathbf{X}^T & \mathbf{Z} \end{bmatrix} \succeq \mathbf{0}_{N+2},
\end{aligned} \tag{16}$$

where $\mathbf{e}_i$ is an M by 1 vector in which the ith element is one and other elements are zero. The solution of (16) and (14) for the source node locations will coincide if the minimum of (16) occurs for $\mathbf{X}$ and $\mathbf{Z}$ such that $\mathbf{Z} = \mathbf{X}^T\mathbf{X}$.

IV. Path Loss Exponent

The PLE determines the rate of RSS attenuation with distance. The value of the PLE depends on the propagation environment and varies typically between 2 (free space) and 4 [1]. In RSS-based localization, the accuracy of the estimate of the source node location highly relies on the PLE value. Generally in wireless localization, first the PLE of the environment is obtained through experimental analysis [36], and then the network is established. However, the value of the PLE might change with time, for instance, due to changes in environment. Therefore, it may be required to calibrate the PLE and collect RSS measurements simultaneously. In [37], the PLE is considered as a nuisance parameter and estimated jointly with the source location. However, in our model, estimating the PLE together with the source location and transmit power appears to be very difficult. In the simulation section, we will examine a condition where the estimators have an imperfect estimate of the PLE and its impact on the performance of proposed algorithms will be presented. Here, we introduce a technique to deal with an inaccurate estimate of the PLE. First, we make an estimate for the PLE (based on the network environment) and compute the source location with the proposed algorithms. Then, we update the value of the PLE as

$$\hat{\boldsymbol{\psi}} = \underset{\boldsymbol{\psi}\in\mathbb{R}^{N+1}}{\arg\min} \sum_{j\in\mathcal{S}} \sum_{i\in\mathcal{A}_j\cup\mathcal{B}_j} \Big(P_{ij} - P_{0j} + 10\beta \log_{10} \hat{d}_{ij}\Big)^2, \tag{17}$$

where $\boldsymbol{\psi} = [\beta;\, \mathbf{p}_0]$ is the unknown vector to be estimated and $\mathbf{p}_0 = [P_{01}, P_{02}, \ldots, P_{0N}]^T$. $\hat{d}_{ij}$ are the estimates of the distances calculated from the estimates of the source node locations. The least squares solution of (17) is obtained as [32, Ch. 4]

$$\hat{\boldsymbol{\psi}} = (\mathbf{B}^T\mathbf{B})^{-1}\mathbf{B}^T\mathbf{p}, \tag{18}$$

where $\mathbf{B} = [\mathbf{b},\, \mathbf{B}_0]$ and

$$\mathbf{p} = \begin{bmatrix} \mathbf{p}_1 \\ \vdots \\ \mathbf{p}_N \end{bmatrix},\ \mathbf{p}_j = \begin{bmatrix} \vdots \\ P_{ij} \\ \vdots \end{bmatrix}_{i\in\mathcal{A}_j\cup\mathcal{B}_j}$$

$$\mathbf{b} = \begin{bmatrix} \mathbf{b}_1 \\ \vdots \\ \mathbf{b}_N \end{bmatrix},\ \mathbf{b}_j = \begin{bmatrix} \vdots \\ -10\log_{10}\hat{d}_{ij} \\ \vdots \end{bmatrix}_{i\in\mathcal{A}_j\cup\mathcal{B}_j}$$

$$\mathbf{B}_0 = \mathrm{diag}\{\mathbf{1}_{n(1)+m(1)}, \ldots, \mathbf{1}_{n(N)+m(N)}\},$$

where $m(j) = |\mathcal{A}_j|$ and $n(j) = |\mathcal{B}_j|$. We estimate $\hat{\beta} = [\hat{\boldsymbol{\psi}}]_1$. Now, the algorithms will be computed with the updated PLE and the iterative procedure continues until the change in $\hat{\beta}$ is sufficiently small. As can be seen in (17), we estimate the transmit powers jointly with the PLE. The main reason is that, in our simulations, we observed that the imperfect PLE causes large error in the estimates of the transmit powers, while the estimates of the source locations suffer less from the imperfect PLE estimate. Hence, when updating the PLE value in (18), we have used the source location estimates but not the transmit power estimates.

V. Complexity Analysis

In this section, we evaluate the computational complexity of the estimators considered in this study based on the total number of floating-point operations or *flops*. The full details of the complexity analysis for each algorithm are given in Appendix C. The complexities are expressed in Appendix C as a function of N, the number of source nodes, M, the number of anchor nodes, and $L = \sum_{j \in \mathcal{S}} |\mathcal{A}_j| + |\mathcal{B}_j|$, the total number of connections. Table I shows the computational complexity of the algorithms for cooperative localization, assuming a network with full connectivity, where $|\mathcal{A}_j| = M$ and $L = N(M + (N-1)/2)$. Table I is obtained by substituting M and $N(M + (N-1)/2)$ for $|\mathcal{A}_j|$ and L respectively in (48), (50), and (52). It should be noted that Table I provides asymptotic complexities of the algorithms, meaning that only the dominating elements are presented. As can be seen, linear estimators (LLS and PLE) require only one iteration. The number of iterations for the SDP algorithm depends on the required accuracy ϵ [25], [38]. The number of iterations for the ML estimator using Gauss-Newton method depends on its initial point and required accuracy [32, Ch. 8]. We will later mention the experimental values for the number of iterations required for each algorithm in the simulation results section. From Table I, we can observe that for a dense network with many source nodes, the complexities per iteration of SDP and ML algorithm are similar but much larger than that of LLS algorithm, however for a modest network size (e.g., 10 source nodes), the complexities per iteration of all algorithms are approximately the same.

VI. Simulation Results

Computer simulations were conducted to evaluate the performance of the proposed algorithms. Two scenarios were examined; in the first scenario, five anchor nodes were placed regularly on the corners

TABLE I
COMPLEXITY OF THE ALGORITHMS FOR COOPERATIVE LOCALIZATION WITH FULL CONNECTIVITY, $|\mathcal{A}_j| = M$, $L = N(M + (N-1)/2)$.
N NUMBER OF SOURCE NODES, M NUMBER OF ANCHOR NODES, L TOTAL NUMBER OF CONNECTIONS.

Algorithm	Iterations	Complexity per Iteration
ML in (12)	k	$O(N^3(M+N/2)^3)$
SDP in (16)	$\sqrt{N}\log(1/\epsilon)$	$O(N^4(M+N/2)^2)$
LLS in (34)	1	$O(6N^3(M+N/2)^2)$
PLE in (18)	1	$O(2N^3(M+N/2)^2)$

and in the center of a square 20 m $\times$ 20 m and ten source nodes were distributed in a square area 19 m $\times$ 19 m inside the convex hull of the anchor nodes. Fig. 2a shows the coordinates of the anchor nodes, source nodes, and reference powers for the first scenario. In the second scenario, the location of the source nodes is the same as in Fig. 2a, but the anchor nodes were placed irregularly. Fig. 2b shows the configuration of the network in the second scenario. The value of the path loss exponent β was known and set to 4, unless otherwise noted. The standard deviation of the shadowing σ_{dB} varied from 1 to 8 dB. The ML estimator was solved by the MATLAB routine `lsqnonlin` using the Levenberg-Marquardt method. The proposed SDP was implemented by the `CVX` toolbox [39] using SeDuMi as the solver [34]. The value of the regularization parameter δ was set to 0.1 for the linear estimator. A summary of the considered algorithms is given in Table II.

TABLE II
THE SUMMARY OF THE CONSIDERED ALGORITHMS.

Algorithm	Description
SDP-URSS	The proposed SDP algorithm in (16) with unknown transmit powers
ML	The ML estimator in (12) initialized with the true values
LLS	The proposed linear estimator in (47)
SDP-UNS	The SDP estimator in [23] with unknown transmit powers
SDP-RSS	The SDP estimator in [13] with true transmit powers
SDP-RSS-WP	The SDP estimator in [13] with -10 dBm reference power assumed for all source nodes
SDP-RSS-P2	The SDP estimator in [13] with 2 dB uncertainty about transmit powers
SDP-RSS-P5	The SDP estimator in [13] with 5 dB uncertainty about transmit powers
ML-SDP-URSS	The ML estimator in (12) initialized with the solution of SDP-URSS
ML-LSS	The ML estimator in (12) initialized with the solution of LLS
ML-RAND	The ML estimator in (12) initialized with random values

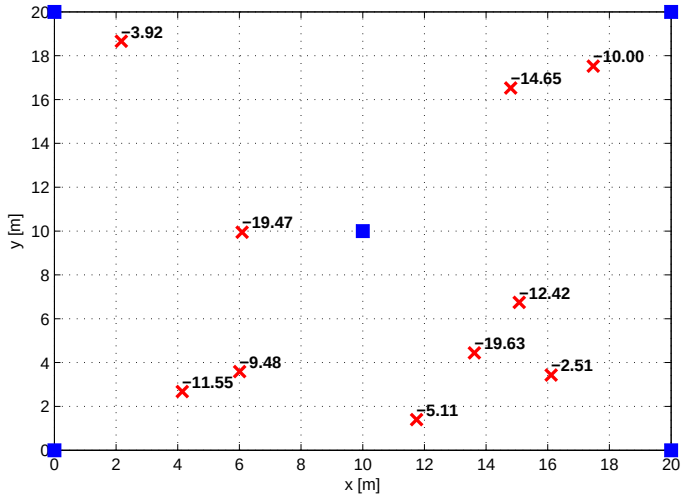

(a) The first scenario

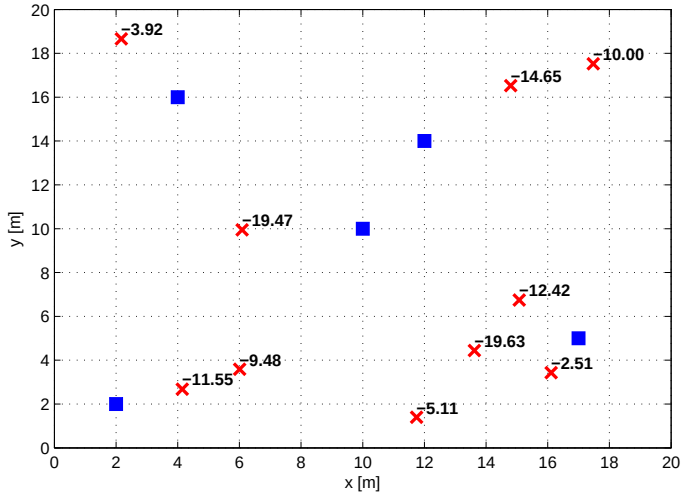

(b) The second scenario

Fig. 2. The configuration the proposed networks. The solid squares and crosses represent the anchor nodes and source nodes, respectively. The value of the reference power, in dBm, for each source node is indicated next to it.

A. Cramér-Rao Lower Bound (CRLB)

In this section, we show the effect of unknown transmit powers on the CRLB accuracy, evaluated on a regular grid. Figs. 3a and 3b show the CRLB ellipse [40] of non-cooperative RSS localization with either known or unknown transmit power when the anchor nodes are placed based on the first and second scenarios, respectively. Fig. 3a illustrates that there is no significant difference between the CRLB of RSS localization with known and unknown transmit power of a source located inside the convex hull of the anchor nodes, whereas, when the source node is relatively close to the anchor nodes or between two

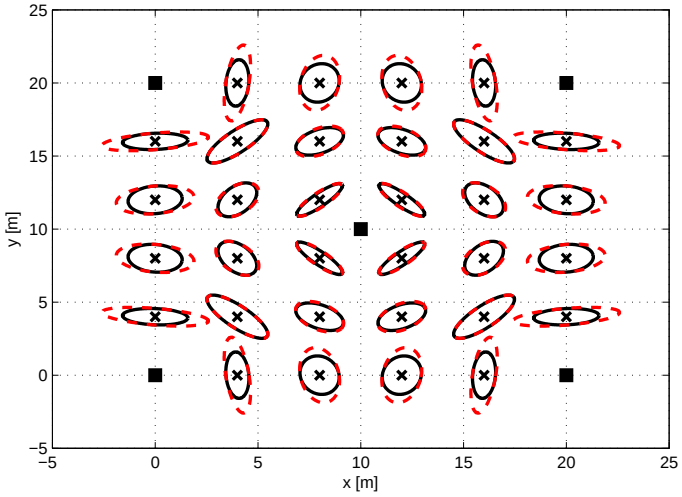

(a) The first scenario

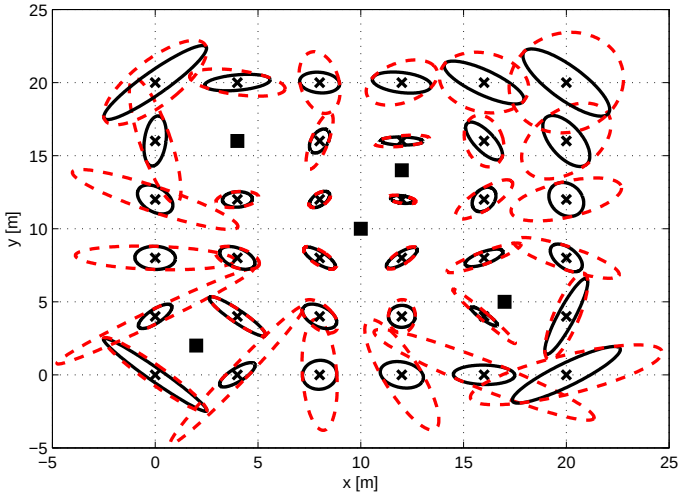

(b) The second scenario

Fig. 3. The CRLB of non-cooperative RSS localization. Black (solid) and red (dashed) circles represent the CRLB ellipse with known transmit power and unknown transmit power, respectively. The solid squares and crosses indicate the anchor nodes and source nodes, respectively. The standard deviation of shadowing term is 3 dB. The difference between the two CRLBs in the second scenario is more significant.

adjacent anchor nodes, the effect of unknown transmit power on the CRLB is more significant. On the other hand, as depicted in Fig. 3b, the differences between the CRLBs for the second scenario are much larger, especially when the source node is located outside the convex hull of the anchor nodes. Thus, when the source node is outside the convex hull, the impact of unknown transmit power is significant. However, the impact is minor when the source node is inside the convex hull. The CRLBs for the cooperative case are more or less similar to the non-cooperative case.

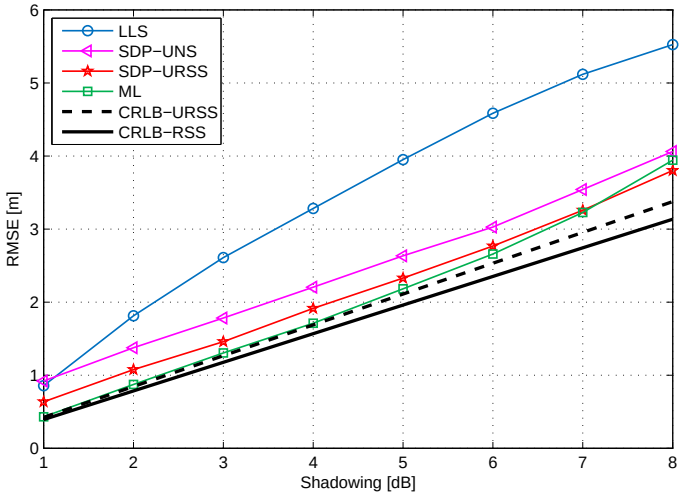

(a) The first scenario

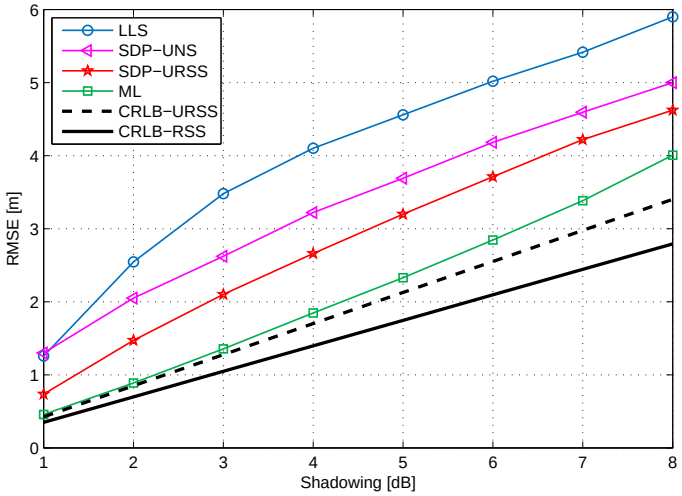

(b) The second scenario

Fig. 4. The RMSE of the proposed algorithms versus the standard deviation of shadowing. The proposed SDP (SDP-URSS) performs very well and its performance is very close to the original ML estimator, especially in regular networks.

B. Root-Mean-Square-Error (RMSE)

Now consider the configuration of the network given in Fig. 2a. Full connectivity was initially assumed, meaning that each source node was connected to all anchor nodes and also to all other source nodes. The locations of the anchor and source nodes were fixed and 500 measurement noise realizations were drawn. The RMSE of each algorithm is calculated by averaging over all estimated source locations and noise realizations. The RMSE performance of the proposed algorithms is depicted in Fig. 4. The solver for the ML estimator was initialized with the true value of the source location. The term URSS is used for RSS

localization when the transmit powers of the source nodes are not known and the term RSS is used for the classic RSS localization with known transmit powers as studied in [2], [13]. CRLB-RSS is the classic CRLB with known transmit powers derived in [13]. As expected, in Fig. 4a the difference between the CRLB with known transmit power in [2] and the CRLB with unknown transmit power is small, since the source nodes were located inside the convex hull of the anchor nodes. Fig. 4a shows that the ML estimator has superior performance for low shadowing standard deviations, but its performance degrades for shadowing standard deviation higher than 5 dB, even though it is initialized with the true values. The proposed SDP (SDP-URSS) performs significantly better than LLS algorithm and is very close to the ML estimator. When shadowing is very high (7 dB and more), the proposed SDP performs slightly better than the ML estimator. The ML estimator is optimal when the number of measurements tends to infinity meaning that no unbiased estimator can have lower RMSE than the ML estimator asymptotically [32, Ch. 7]. However, here the number of measurements is limited, therefore, the optimality of the ML estimator is not guaranteed. Moreover, since both the ML estimator [2] and the proposed SDP are biased (especially when either the number of measurements is limited or shadowing is high), we cannot expect that the ML estimator provides the best accuracy. Note that this behavior has also been observed in [13]. Besides the proposed algorithms, an SDP algorithm given in [23] (labeled as SDP-UNS) is also included in the simulations. It should be noted that SDP-UNS is generally based on the fact that the transmit powers are available. Therefore, we modified the algorithm to estimate jointly transmit powers and source locations. There are many weighting terms in SDP-UNS which depend highly on the transmit powers [23]. To rectify this problem, we first set the value of the weighting terms to 1 and estimate transmit powers and source locations. Then, we updated the weighting terms using the estimated transmit powers and ran the algorithm again. The performance of SDP-UNS falls between LLS and SDP-URSS, even though its computational complexity is higher than SDP-URSS.

The comparison of the proposed algorithms versus the standard deviation of shadowing for the second scenario is illustrated in Fig. 4b. Here, there is a considerable gap between CRLB-RSS and CRLB-URSS. The performance order of the algorithms is the same as in the first scenario. In comparison with the previous scenario, the difference between the accuracy of the ML estimator and the proposed SDP is larger. However, the proposed SDP-URSS is still much better than LLS and SDP-UNS estimators.

In Table III, we compare the average running time of the considered algorithms. The running time

TABLE III
THE AVERAGE RUNNING TIME OF THE CONSIDERED ALGORITHMS.
$N = 10$, $|\mathcal{A}_j| = 5, L = 95$.
CPU: INTEL CORE 2 DUO E7500 2.93 GHZ

Algorithm	Iterations	Time [ms]
ML	22	268.72
SDP-URSS	19	218.34
SDP-UNS	35	462.16
LLS	1	11.81

is measured by averaging over 500 noise realizations when the first network with full connectivity is considered and the standard deviation of the shadowing is set to 3 dB. LLS has the lowest complexity and therefore the fastest running time. The required running time of the proposed SDP-URSS is about 20% lower than the ML estimator. From Table I, the complexity per iteration for all algorithms is almost identical for this network size ($N = 10, |\mathcal{A}_j| = 5$). However, they require different numbers of iterations. Moreover, we empirically computed the average number of iterations for the ML and SDP algorithms. The average number of iterations for the ML and SDP-URSS were 22 and 19, respectively. Consequently, the running time of the ML and SDP-URSS is approximately 22 and 19 times higher than LLS (which requires only one iteration). As mentioned in Section V, the running time of the ML estimator depends highly on the initialization. Here, the ML estimator has been initialized with the true values which cuts down its running time and improves its performance. Later, we will discuss the effect of initialization on the complexity and performance of the ML estimator. The computational of complexity of SDP-UNS in [23] is almost the same as that of the proposed SDP-URSS. However, as mentioned above, SDP-UNS should be run twice because of the estimation of the weighting terms. Therefore, the required running time of SDP-UNS is nearly as twice as that of SDP-URSS. Thus, complexity and performance are directly related for the considered algorithms, except for SDP-UNS which was designed for known transmit powers.

Fig. 5 illustrates the performance of the proposed SDP compared with the previously studied algorithm in [13] (labeled as SDP-RSS) for the first scenario. Since SDP-RSS is based on the availability of source transmit powers, the true values of the source nodes transmit powers were given to SDP-RSS in Fig. 5. In SDP-RSS-WP, the same algorithm in [13] was used, however, the algorithm did not have the exact value of the transmit powers and the value of -10 dBm was given to the algorithm as the reference power

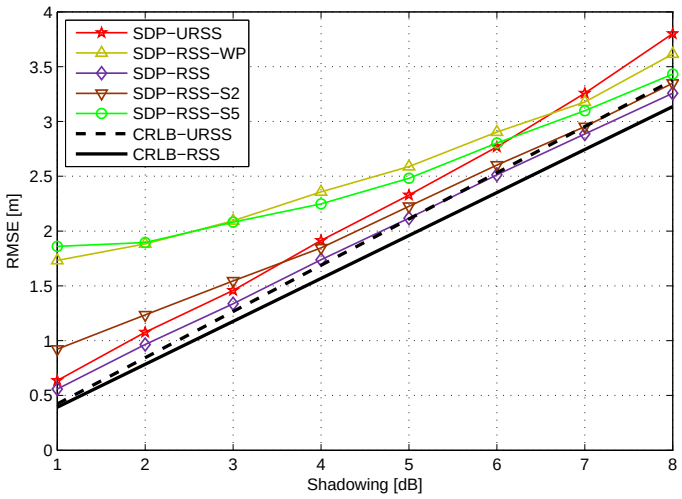

Fig. 5. The RMSE of the proposed algorithms versus the standard deviation of shadowing for the first scenario with uncertainty in the transmit power. Although in the first scenario unknown transmit powers do not have a huge impact on the CRLB accuracy, employing the proposed SDP (handling unknown transmit powers) is very useful and strongly improves performance.

for all source nodes. We also proposed a condition where there is uncertainty about the transmit power. Assume that approximate values of the transmit powers, $\bar{P}_{0j}$, are given as

$$\bar{P}_{0j} = P_{0j} + v_j, \tag{19}$$

where $v_j \sim \mathcal{N}(0,\, \sigma_{P_0})$ are Gaussian random variables with standard deviation σ_{P_0}. Instead of the true value of transmit power P_{0j}, the value of $\bar{P}_{0j}$ was given to the SDP algorithm in [13]. In this simulation, the value of σ_{P_0} was set to 2 and 5 dB for SDP-RSS-S2 and SDP-RSS-S5, respectively. SDP-RSS (exact knowledge) outperforms the proposed approach, mainly because the true value of transmit power is available to it. SDP-RSS-S2 performs worse than SDP-RSS especially when the shadowing is low. SDP-RSS-WP and SDP-RSS-S5 have poor performance for $\sigma_{dB} < 6dB$. As can be seen, as the standard deviation of the shadowing increases, the effect of transmit power uncertainty on the estimation accuracy decreases since performance is dominated by shadowing. The performance of the proposed SDP-URSS is close to SDP-RSS and has better accuracy than SDP-RSS-S5 and SDP-RSS-WP, especially for low shadowing standard deviation. Hence, although in the first scenario, unknown transmit powers do not have a huge impact on the CRLB, employing an algorithm handling this uncertainty is very useful and strongly improves performance.

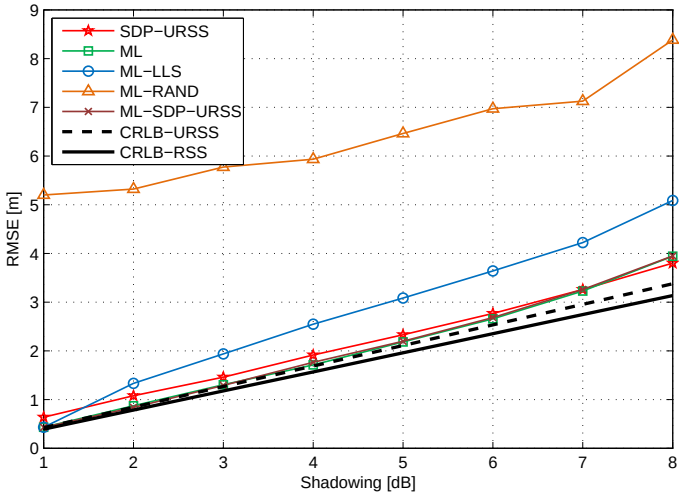

(a) The first scenario

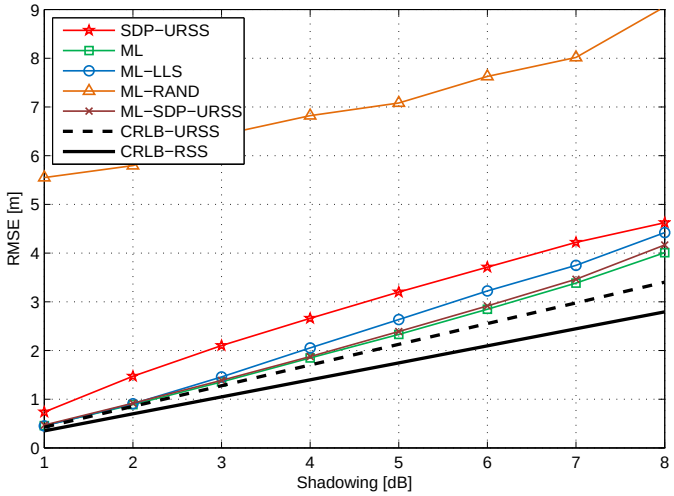

(b) The second scenario

Fig. 6. The RMSE of proposed algorithms versus the standard deviation of shadowing and different initializations for the ML estimator. The initialization has a huge impact on the ML estimator performance. The proposed SDP algorithm provides a suitable initial point for the ML estimator if better accuracy is required.

C. Initialization

It is well-known that the performance of the ML estimator depends heavily on its initial solution, since most implementations of the ML estimator are iterative. To further compare the proposed SDP and the ML estimator, we initialized the solver of the ML estimator with different values. Fig. 6a and 6b illustrate the RMSE of the proposed algorithms as a function of the standard deviation of the shadowing with different initial points for the solver of the ML estimator for the first and second scenarios, respectively. The curve labeled as ML stands for the ML estimator initialized with the true values, whereas ML-SDP, ML-LLS,

TABLE IV
THE AVERAGE RUNNING TIME OF THE ML ESTIMATOR WITH DIFFERENT INITIALIZATIONS.

Algorithm	Iterations	Time [ms]
ML	22	268.72
ML-SDP	23	282.51
ML-LLS	26	316.16
ML-RAND	43	514.58

and ML-RAND stand for the ML estimator when its solver was initialized with the SDP solution, LLS solution, and random values, respectively. Fig. 6 shows that in both scenarios, the ML estimator initialized with the true values outperforms other algorithms as expected. However, the initial point can have a large effect on ML accuracy. The proposed SDP algorithm offers better performance compared to ML-LLS and ML-RAND, especially for large shadow fading standard deviation. It is interesting that when the ML estimator is initialized with the solution of the proposed SDP (ML-SDP-URSS), we can achieve almost the same accuracy as the ML algorithm initialized with the true solution. Therefore, although the proposed SDP algorithm has excellent standalone performance, it can also be used as an initial point for the ML estimator when even better accuracy is required. Fig. 6 also shows that randomly initializing the ML estimator yields extremely poor performance even at low σ_{dB} values. Table IV shows the running time of the ML estimator for different initializations. We can see that the initial point has a huge impact on not only the performance of the ML estimator, but also the required number of iterations and the running time. When the initial point is not sufficiently close to the global minimum, the number of iterations increases significantly. Moreover, there is no guarantee that the algorithm converges to the global minimum. This is the major drawback of the ML estimator. In this case, an increase in running time (complexity) does not result in performance improvement because of initialization; in fact the opposite is true.

D. Connectivity

In the previous simulations, we assumed that the network has full connectivity. However, this assumption is not valid in all practical cases where the connections among sensors are limited. In this section, we examine the first scenario but with limited connectivity. Fig. 7 shows the RMSE of the proposed algorithms versus the number of connections when the shadowing standard deviation is 4 dB. For instance, the value of 10 on the x-axis means that each source node is connected to the 10 closest sensors, either anchor nodes or source nodes. The LLS estimator in (47) is no longer applicable here

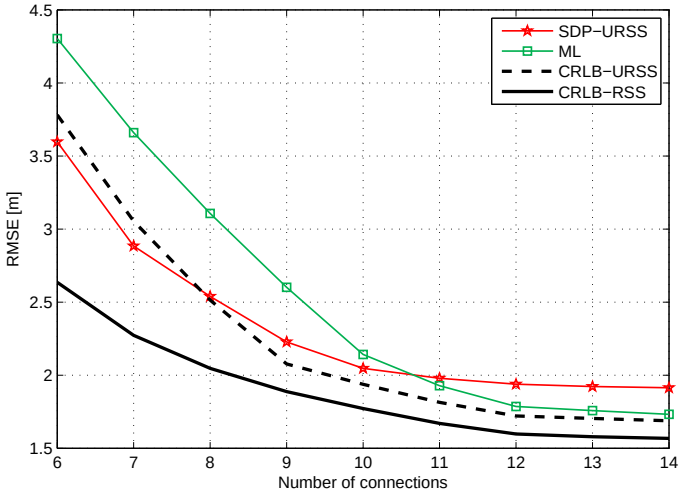

Fig. 7. The RMSE of the proposed algorithms versus the number of connections. The standard deviation of the shadowing is 4 dB. As the number of connections increases, the estimation accuracy improves. The proposed SDP algorithm has better performance than the ML estimator when the connectivity in the network is limited.

because in its formulation, each source node should be connected to at least four noncollinear anchor nodes, but in low connectivity there is no guarantee that each source node can communicate with four neighboring anchor nodes. Fig. 7 shows that by increasing the number of connections, the estimation accuracy improves, as expected. Comparing the two CRLBs, we observe that the unknown transmit power has more effect on the CRLB accuracy when the network connectivity is limited. The proposed SDP performs better than the ML estimator when the number of connections in the network is very low. Potential reasons were previously mentioned in the description of Fig. 4. When the number of connections is 6 or 7, the proposed SDP is slightly lower than CRLB. As mentioned previously in Section VI-B, both SDP-URSS and ML estimators are biased (especially when the number of connections is limited) and thus the CRLB cannot provide an absolute lower bound for them [2], [13], [41].

E. Path Loss Exponent (PLE)

In this section, we investigate the effect of imperfect PLE knowledge on the performance of the proposed algorithms. The first scenario was considered for this simulation. However, we assume that the estimators do not have the exact value of the PLE and instead they have an approximate value modeled as

$$\bar{\beta} = \beta + \mathcal{N}(0,\, 1), \tag{20}$$

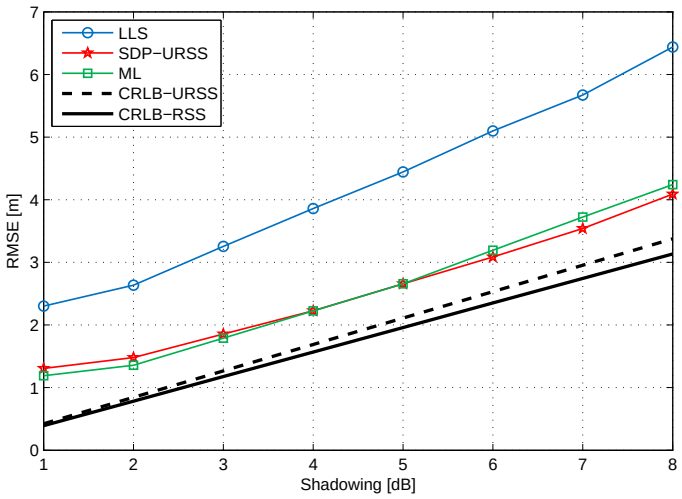

Fig. 8. The RMSE of the proposed algorithms versus the standard deviation of shadowing for the first scenario with uncertainty in the PLE. Imperfect PLE decreases the performance of all algorithms, especially at low σ_{dB} values. When the shadowing is larger than 6 dB, the proposed SDP is more robust against imperfect PLE than the ML estimator.

where $\beta = 4$ in our simulations. Fig. 8 shows the performance of the proposed algorithms in this condition. The order of the algorithms remains unchanged compared to Fig. 4a. It is obvious that the performance of all the algorithms degrades, especially at low values of σ_{dB}. The proposed SDP-URSS performs better than the ML estimator in the presence of PLE uncertainty when the shadowing standard deviation is larger than 5 dB. Now, assume that we have an imperfect value of the PLE and the proposed algorithms are computed based on the approach given in (18). Fig. 9 shows the estimate of the PLE versus the number of iterations and different shadowing standard deviations for the proposed SDP in (16). The true value of the PLE was set to 4 and we started the algorithm with the PLE of 3 and 5. It can be seen from Fig. 8 that the RMSE performance of the proposed algorithms is poor at the low shadowing standard deviations. However, as depicted in Fig. 9, by exploiting the iterative approach given in (18), the imperfect PLE estimate converges to a value very close to the true value for a small number of iterations. It is worth mentioning that we have only plotted the convergence of the PLE for the proposed SDP in (16). However, the PLE convergence for the ML and LLS algorithms is more or less the same. Our simulations show that once the PLE has converged, the RMSE of the proposed algorithms for the source locations is almost identical to Fig. 4a.

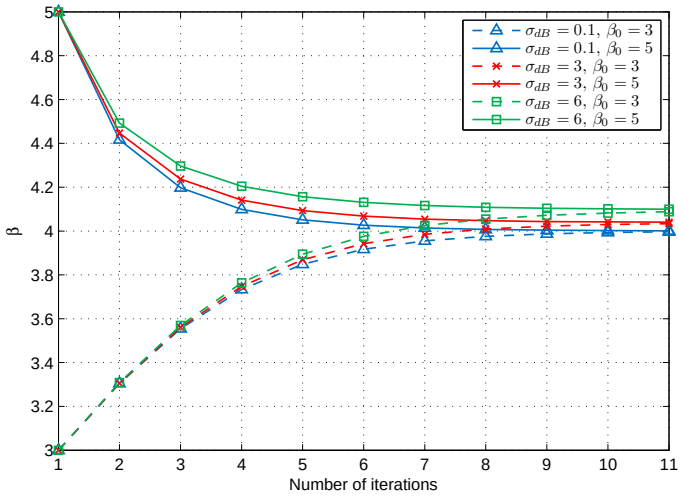

Fig. 9. The convergence rate of the PLE for the proposed SDP. The algorithm starts with the initial value β_0. The true value of β is 4. Once the PLE has converged, the proposed algorithms achieve performance nearly identical to what is achieved with perfect knowledge.

VII. Conclusion

In this paper, cooperative RSS-based sensor localization with unknown and different transmit powers was examined. The CRLB of the measurement model was derived and through computer simulations it was shown that the effect of unknown transmit powers on the CRLB accuracy of the source locations depends strongly on the network deployment geometry. A novel SDP technique was derived to estimate the source transmit powers jointly with the source node locations. The complexity analyses of the considered algorithms were presented. Simulation results demonstrated that the proposed SDP algorithm has excellent performance, close to the original ML estimator in most conditions. Not only does the proposed SDP exhibit good accuracy alone but also gives a good initial point for the ML estimator if further refinement is required. We also introduced an approach for dealing with imperfect information about the path loss exponent which can strongly impact the performance of RSS-based localization algorithms.

Acknowledgment

The authors would like to thank the associate editor, Prof. K. C. Ho, and the anonymous reviewers for their valuable comments and suggestions which improved the quality of the paper.

APPENDIX A
CRAMÉR-RAO LOWER BOUND OF COOPERATIVE RSS LOCALIZATION

In this section, the CRLB of cooperative RSS localization with unknown transmit power is derived. The CRLB defines a lower bound on the variance of any unbiased estimator and is employed as a benchmark for evaluating the performance of estimators [32, Ch. 3], [1], [2], [13]. Since the transmit power of the source nodes is not available to the estimator, it should also be taken into account as an unknown parameter. Let us recall the vector of unknown parameters $\boldsymbol{\phi} = [\mathbf{x}^T, \mathbf{p}_0^T]^T$ including the source node locations $\mathbf{x} = [\mathbf{x}_1^T, \mathbf{x}_2^T, \ldots, \mathbf{x}_N^T]^T$ and the source node transmit powers $\mathbf{p}_0 = [P_{01}, P_{02}, \ldots, P_{0N}]^T$. From the measurement model in (11), the logarithm of the probability density function of the RSS measurements is written as

$$\ln p(\mathbf{p}; \boldsymbol{\phi}) = k - \sigma_{dB}^{-2}(\boldsymbol{\mu}(\boldsymbol{\phi}) - \mathbf{p})^T(\boldsymbol{\mu}(\boldsymbol{\phi}) - \mathbf{p}), \tag{21}$$

where k is a constant which does not depend on the unknown parameters and $\mathbf{p}$ is the measurement vector defined in (18). $\boldsymbol{\mu}(\boldsymbol{\phi})$ is the mean of the measurement vector $\mathbf{p}$ defined as

$$\boldsymbol{\mu}(\boldsymbol{\phi}) = \begin{bmatrix} \boldsymbol{\mu}_1(\boldsymbol{\phi}) \\ \vdots \\ \boldsymbol{\mu}_N(\boldsymbol{\phi}) \end{bmatrix}, \ \boldsymbol{\mu}_j(\boldsymbol{\phi}) = \begin{bmatrix} \vdots \\ \mu_{ij} \\ \vdots \end{bmatrix}_{i \in \mathcal{A}_j \cup \mathcal{B}_j} \tag{22}$$

where

$$\mu_{ij} = P_{0j} - 10\beta \log_{10} d_{ij}.$$

The CRLB of the unknown parameters are the diagonal elements of the inverse of the Fisher information matrix [32, Ch. 3]. The Fisher information matrix of the measurement model in (11) is obtained as [32, Ch. 3]

$$\mathbf{J}(\boldsymbol{\phi}) = \sigma_{dB}^{-2}\mathbf{F}^T\mathbf{F}, \tag{23}$$

where

$$\mathbf{F} = \frac{\partial \boldsymbol{\mu}(\boldsymbol{\phi})}{\partial \boldsymbol{\phi}} = \begin{bmatrix} \mathbf{F}_1 \\ \vdots \\ \mathbf{F}_N \end{bmatrix}, \ \mathbf{F}_j = \begin{bmatrix} \vdots \\ \mathbf{f}_{ij} \\ \vdots \end{bmatrix}_{i \in \mathcal{A}_j \cup \mathcal{B}_j}$$

and $\mathbf{f}_{ij} = [\mathbf{f}_{ij}^{y},\ \mathbf{f}_{ij}^{p}]$,

$$\begin{aligned}
\mathbf{f}_{ij}^{y} &= \Big[\mathbf{0}_{1\times 2(j-1)}, \mathbf{u}_{ij}^{T}, \mathbf{0}_{1\times 2(N-j)}\Big],\ i \in \mathcal{A}_j \\
\mathbf{f}_{ij}^{y} &= \Big[\mathbf{0}_{1\times 2(j-1)}, \mathbf{u}_{ij}^{T}, \mathbf{0}_{1\times 2(i-j-1)}, -\mathbf{u}_{ij}^{T}, \mathbf{0}_{1\times 2(N-i)}\Big],\ i \in \mathcal{B}_j \\
\mathbf{f}_{ij}^{p} &= \Big[\mathbf{0}_{1\times (j-1)}, 1, \mathbf{0}_{1\times (N-j)}\Big],\ i \in \mathcal{A}_j \cup \mathcal{B}_j \\
\mathbf{u}_{ij} &= \frac{10\beta}{\ln 10}\frac{(\mathbf{y}_i - \mathbf{x}_j)}{d_{ij}^2},\ i \in \mathcal{A}_j \\
\mathbf{u}_{ij} &= \frac{10\beta}{\ln 10}\frac{(\mathbf{x}_i - \mathbf{x}_j)}{d_{ij}^2},\ i \in \mathcal{B}_j.
\end{aligned}$$

Therefore, the CRLB of the unknown parameters $\boldsymbol{\phi}$ is computed as

$$\text{CRLB}([\boldsymbol{\phi}]_r) = \left[\mathbf{J}^{-1}(\boldsymbol{\phi})\right]_{r,r}, \quad r = 1, 2, \ldots, 3N. \tag{24}$$

APPENDIX B
LINEAR ESTIMATOR FOR COOPERATIVE RSS LOCALIZATION

In this work, we derived an SDP estimator to deal with the convergence problem of the ML estimator and its complexity. Another solution for the ML convergence problem is to use a linear estimator which has an analytical closed-form solution. To obtain a linear estimator, some approximations should be applied to linearize the nonlinear measurement model of (1). Linear estimators for RSS localization have been previously considered in the literature [4]. However, to the best of our knowledge, all of them are based on availability of the transmitted power. Here, we derive a similar technique to the one used in [4] with considering unknown transmit powers. Since linearizing the source-source measurements is difficult, we propose a two-step algorithm. In the first step (called coarse estimation), we estimate the location of each source node independently using only source-anchor measurements. Then, in the next step (called fine estimation), we improve the accuracy of the estimated source locations by using source-source measurements. The main drawback of this approach is that we require at least four source-anchor measurements for each source node, otherwise we cannot find a coarse estimate for the source location in the first step and therefore the second step will be not applicable. We now start by describing the first step. Let us rewrite (7) for cooperative localization as ($j \in \mathcal{S}$)

$$h_{ij}\lambda_{ij} = \alpha_j + \epsilon_{ij}, \quad i \in \mathcal{A}_j, \tag{25}$$

where $\epsilon_{ij} = -n_{ij}\alpha_j(\ln 10)/5\beta$ is a zero-mean Gaussian random variable with variance $(\ln 10)^2\alpha_j^2\sigma_{dB}^2/25\beta^2$. Expanding the left-hand side (LHS) of (25) and rearranging gives

$$2\lambda_{ij}\mathbf{y}_i^T\mathbf{x}_j - \lambda_{ij}\mathbf{x}_j^T\mathbf{x}_j + \alpha_j = \lambda_{ij}\mathbf{y}_i^T\mathbf{y}_i + \epsilon_{ij}, \quad i \in \mathcal{A}_j. \tag{26}$$

Let $\boldsymbol{\theta}_{1,j} = [\mathbf{x}_j^T, \mathbf{x}_j^T\mathbf{x}_j, \alpha_j]^T$ be the unknown vector to be estimated. Then (26) can be expressed in matrix form as

$$\mathbf{G}_{1,j}\boldsymbol{\theta}_{1,j} = \mathbf{h}_{1,j} + \boldsymbol{\epsilon}_{1,j}, \tag{27}$$

where

$$\mathbf{G}_{1,j} = \begin{bmatrix} \vdots & \vdots & \vdots \\ 2\lambda_{ij}\mathbf{y}_i^T & -\lambda_{ij} & 1 \\ \vdots & \vdots & \vdots \end{bmatrix},$$

$$\mathbf{h}_{1,j} = \begin{bmatrix} \vdots \\ \lambda_{ij}\mathbf{y}_i^T\mathbf{y}_i \\ \vdots \end{bmatrix}, \quad \boldsymbol{\epsilon}_{1,j} = \begin{bmatrix} \vdots \\ \epsilon_{ij} \\ \vdots \end{bmatrix}, \ i \in \mathcal{A}_j \cup \mathcal{B}_j.$$

The LLS solution of (27) is [32, Ch. 4]

$$\hat{\boldsymbol{\theta}}_{1,j} = (\mathbf{G}_{1,j}^T\mathbf{W}_{1,j}\mathbf{G}_{1,j})^{-1}\mathbf{G}_{1,j}^T\mathbf{W}_{1,j}\mathbf{h}_{1,j}, \tag{28}$$

where $\mathbf{W}_{1,j}$ is the weighting matrix which is the inverse of the covariance matrix of the residual error vector $\boldsymbol{\epsilon}_{1,j}$

$$\mathbf{W}_{1,j} = \mathrm{E}[\boldsymbol{\epsilon}_{1,j}\boldsymbol{\epsilon}_{1,j}^T]^{-1} = ((\ln 10)\alpha_j\sigma_{dB}/5\beta)^{-2}\,\mathbf{I}_{m(j)}. \tag{29}$$

where $m(j) = |\mathcal{A}_j|$. The covariance matrix of the estimated vector $\hat{\boldsymbol{\theta}}_{1,j}$ is [32, Ch. 4]

$$\mathbf{C}_{\hat{\theta}_{1,j}} = (\mathbf{G}_{1,j}^T\mathbf{W}_{1,j}\mathbf{G}_{1,j})^{-1}. \tag{30}$$

The weighting matrix $\mathbf{W}_{1,j}$ depends on the unknown parameter α_j. Therefore, to compute the weighting matrix, we can eliminate the value of α_j in (29) and determine the solution of (28). Since α_j is a constant factor in $\mathbf{W}_{1,j}$, its value does not change the solution of $\hat{\boldsymbol{\theta}}_{1,j}$ in (28). However, for further computations, we can calculate the weighting matrix $\mathbf{W}_{1,j}$ approximately by $\hat{\alpha}_j$ obtained from (28).

Since the elements of estimated parameters in (28) are dependent, one method to improve the estimation accuracy, called correction technique [5], [17], [42], is to take this relation between elements of $\hat{\boldsymbol{\theta}}_{1,j}$ into account. Here we extend the correction technique to our problem. The unknown vector $\boldsymbol{\theta}_{1,j}$ can be expressed as

$$\hat{\boldsymbol{\theta}}_{1,j} = \boldsymbol{\theta}_{1,j} + \Delta\boldsymbol{\theta}_{1,j}, \tag{31}$$

where $\Delta\boldsymbol{\theta}_{1,j}$ is the estimation error. Squaring the first two elements of (31) (element-wise) yields

$$\begin{aligned}
[\hat{\boldsymbol{\theta}}_{1,j}]_1^2 &= [\boldsymbol{\theta}_{1,j}]_1^2 + 2[\boldsymbol{\theta}_{1,j}]_1[\Delta\boldsymbol{\theta}_{1,j}]_1 + [\Delta\boldsymbol{\theta}_{1,j}]_1^2 \\
&\simeq [\boldsymbol{\theta}_{1,j}]_1^2 + 2[\boldsymbol{\theta}_{1,j}]_1[\Delta\boldsymbol{\theta}_{1,j}]_1, \\
[\hat{\boldsymbol{\theta}}_{1,j}]_2^2 &= [\boldsymbol{\theta}_{1,j}]_2^2 + 2[\boldsymbol{\theta}_{1,j}]_2[\Delta\boldsymbol{\theta}_{1,j}]_2 + [\Delta\boldsymbol{\theta}_{1,j}]_2^2 \\
&\simeq [\boldsymbol{\theta}_{1,j}]_2^2 + 2[\boldsymbol{\theta}_{1,j}]_2[\Delta\boldsymbol{\theta}_{1,j}]_2,
\end{aligned} \tag{32}$$

where we assume that the estimation error $\Delta\boldsymbol{\theta}_{1,j}$ is sufficiently small. Now, consider the following expressions [17]

$$\mathbf{G}_2\boldsymbol{\theta}_{2,j} = \mathbf{h}_{2,j} + \boldsymbol{\epsilon}_{2,j}, \tag{33}$$

where $\boldsymbol{\theta}_{2,j} = [a_j^2, b_j^2, \alpha_j]^T$ and

$$\mathbf{G}_2 = \begin{bmatrix} 1 & 0 & 0 \\ 0 & 1 & 0 \\ 1 & 1 & 0 \\ 0 & 0 & 1 \end{bmatrix}, \ \mathbf{h}_{2,j} = \begin{bmatrix} [\hat{\boldsymbol{\theta}}_{1,j}]_1^2 \\ [\hat{\boldsymbol{\theta}}_{1,j}]_2^2 \\ [\hat{\boldsymbol{\theta}}_{1,j}]_3 \\ [\hat{\boldsymbol{\theta}}_{1,j}]_4 \end{bmatrix}, \ \boldsymbol{\epsilon}_{2,j} = -\mathbf{B}_j\Delta\boldsymbol{\theta}_{1,j},$$

and $\mathbf{B}_j = \mathrm{diag}\{2[\boldsymbol{\theta}_{1,j}]_1, 2[\boldsymbol{\theta}_{1,j}]_2, 1, 1\}$. The LLS solution of (33) is [32, Ch. 4]

$$\hat{\boldsymbol{\theta}}_{2,j} = (\mathbf{G}^T\mathbf{W}_{2,j}\mathbf{G})^{-1}\mathbf{G}^T\mathbf{W}_{2,j}\mathbf{h}_{2,j}, \tag{34}$$

where $\mathbf{W}_{2,j}$ is the weighting matrix equal to the inverse of the covariance matrix of the residual error vector $\boldsymbol{\epsilon}_{2,j}$

$$\mathbf{W}_{2,j} = \mathrm{E}[\boldsymbol{\epsilon}_{2,j}\boldsymbol{\epsilon}_{2,j}^T]^{-1} = \left(\mathbf{B}_j^T\mathbf{C}_{\hat{\theta}_{1,j}}\mathbf{B}_j\right)^{-1}, \tag{35}$$

where $\mathbf{C}_{\hat{\theta}_{1,j}}$ is computed in (30). It should be noted that the weighting matrix $\mathbf{W}_{2,j}$ depends on the

unknown parameters $\boldsymbol{\theta}_1$. Therefore, the weighting matrix is approximately calculated by available $\hat{\boldsymbol{\theta}}_1$ rather than $\boldsymbol{\theta}_1$. Our simulations show that the accuracy degradation due to the approximation is not significant. The covariance matrix of the estimated vector $\hat{\boldsymbol{\theta}}_{2,j}$ is [32, Ch. 4]

$$\mathbf{C}_{\hat{\theta}_{2,j}} = (\mathbf{G}_2^T \mathbf{W}_{2,j} \mathbf{G}_2)^{-1}. \tag{36}$$

Finally, the estimation of the source location $\hat{\mathbf{x}}_j = [\hat{a}_j, \hat{b}_j]^T$ is [17], [18], [43]

$$\begin{aligned} \hat{a}_j &= \mathrm{sgn}([\hat{\boldsymbol{\theta}}_{1,j}]_1)\sqrt{|[\hat{\boldsymbol{\theta}}_{2,j}]_1|} \\ \hat{b}_j &= \mathrm{sgn}(|[\hat{\boldsymbol{\theta}}_{1,j}]_2|)\sqrt{|[\hat{\boldsymbol{\theta}}_{2,j}]_2|}, \end{aligned} \tag{37}$$

where $\mathrm{sgn}(z) = z/|z|$ is the sign function. The covariance matrix of the estimated source location $\hat{\mathbf{x}}_j$ is computed as [18], [43]

$$\mathbf{C}_{\hat{\mathbf{x}}_j} = \mathbf{D}_j^T [\mathbf{C}_{\hat{\theta}_{2,j}}]_{1:2,1:2} \mathbf{D}_j, \tag{38}$$

where $\mathbf{D}_j = \frac{1}{2}\mathrm{diag}\{|a_j|^{-1}, |b_j|^{-1}\}$ and $[\mathbf{A}]_{1:n,1:m}$ denotes the upper-left $n \times m$ part of matrix $\mathbf{A}$.

Now we continue describing the second step using both source-source and source-anchor measurements. The relationships between the estimated and the true value of the source location and the transmit power of the source node are

$$\begin{aligned} \mathbf{x}_j &= \hat{\mathbf{x}}_j - \Delta\mathbf{x}_j, \\ P_{0j} &= \hat{P}_{0j} - \Delta P_{0j}, \end{aligned} \tag{39}$$

where $\hat{P}_{0j} = 5\beta \log_{10}(\hat{\alpha}_j)$ ($\hat{\alpha}_j = [\hat{\boldsymbol{\theta}}_{2,j}]_3$ is computed for each source node from (34)), $\Delta\mathbf{x}_j$ and ΔP_{0j} are the estimation error of the source location and the source transmit power, respectively. Equation (11) is a function of the unknown parameters $\mathbf{x}_j$ and P_{0j}. We substitute (39) for $\mathbf{x}_j$ and P_{0j} in (11). Therefore, ΔP_{0j} and $\Delta\mathbf{x}_j$ are the new unknown parameters to be estimated in (11).

$$\begin{aligned} P_{ij} &= (\hat{P}_{0j} - P_{0j}) \\ &\quad - 10\beta \log_{10} \|\mathbf{y}_i - (\hat{\mathbf{x}}_j - \Delta\mathbf{x}_j)\| + n_{ij},\ i \in \mathcal{A}_j, \\ P_{ij} &= (\hat{P}_{0j} - \Delta P_{0j}) \\ &\quad - 10\beta \log_{10} \|(\hat{\mathbf{x}}_i - \Delta\mathbf{x}_i) - (\hat{\mathbf{x}}_j - \Delta\mathbf{x}_j)\| + n_{ij},\ i \in \mathcal{B}_j. \end{aligned} \tag{40}$$

Taking the power of 10 on both sides of (40) and rearranging yields

$$\hat{\xi}_{ij}\Delta\alpha_j 10^{n_{ij}/10\beta} = \|\mathbf{y}_i - (\hat{\mathbf{x}}_j - \Delta\mathbf{x}_j)\|,\ i \in \mathcal{A}_j, \tag{41}$$
$$\hat{\xi}_{ij}\Delta\alpha_j 10^{n_{ij}/10\beta} = \|(\hat{\mathbf{x}}_i - \Delta\mathbf{x}_i) - (\hat{\mathbf{x}}_j - \Delta\mathbf{x}_j)\|,\ i \in \mathcal{B}_j,$$

where $\hat{\xi}_{ij} \triangleq 10^{(\hat{P}_{0j} - P_{ij})/10\beta}$ and $\Delta\alpha_j \triangleq 10^{-\Delta P_{0j}/10\beta}$. By using the first-order Taylor series approximation for the third element of the LHS and the element of the RHS, (41) turns into

$$\hat{\xi}_{ij}\Delta\alpha_j(1 + \frac{\ln 10}{10\beta}n_{ij}) = \hat{d}_{ij} - \hat{\mathbf{u}}_{ij}^T\Delta\mathbf{x}_j,\ i \in \mathcal{A}_j, \tag{42}$$
$$\hat{\xi}_{ij}\Delta\alpha_j(1 + \frac{\ln 10}{10\beta}n_{ij}) = \hat{d}_{ij} - \hat{\mathbf{u}}_{ij}^T\Delta\mathbf{x}_j + \hat{\mathbf{u}}_{ij}^T\Delta\mathbf{x}_i,\ i \in \mathcal{B}_j,$$

where

$$\hat{\mathbf{u}}_{ij} = \frac{(\hat{\mathbf{x}}_j - \mathbf{y}_i)}{\hat{d}_{ij}},\ \hat{d}_{ij} = \|\mathbf{y}_i - \hat{\mathbf{x}}_j\|,\ i \in \mathcal{A}_j,$$
$$\hat{\mathbf{u}}_{ij} = \frac{(\hat{\mathbf{x}}_j - \hat{\mathbf{x}}_i)}{\hat{d}_{ij}},\ \hat{d}_{ij} = \|\hat{\mathbf{x}}_i - \hat{\mathbf{x}}_j\|,\ i \in \mathcal{B}_j.$$

Rearranging (42) gives

$$\hat{\mathbf{u}}_{ij}^T\Delta\mathbf{x}_j + \hat{\xi}_{ij}\Delta\alpha_j = \hat{d}_{ij} + \epsilon_{ij}, \qquad i \in \mathcal{A}_j,$$
$$-\hat{\mathbf{u}}_{ij}^T\Delta\mathbf{x}_i + \hat{\mathbf{u}}_{ij}^T\Delta\mathbf{x}_j + \hat{\xi}_{ij}\Delta\alpha_j = \hat{d}_{ij} + \epsilon_{ij}, \qquad i \in \mathcal{B}_j, \tag{43}$$

where $\epsilon_{ij} \triangleq (\ln 10)\,\hat{\xi}_{ij}\Delta\alpha_j n_{ij}/10\beta$. Let $\Delta\boldsymbol{\theta}_3 = [\Delta\mathbf{x}_1^T, \ldots, \Delta\mathbf{x}_N^T, \Delta\alpha_1, \ldots, \Delta\alpha_N]^T$ be unknown parameters to be estimated. We can write (43) in matrix form as

$$\mathbf{G}_3\Delta\boldsymbol{\theta}_3 = \mathbf{h}_3 + \boldsymbol{\epsilon}_3, \tag{44}$$

where

$$\mathbf{G}_3 = \begin{bmatrix} \mathbf{G}_{3,1} \\ \vdots \\ \mathbf{G}_{3,N} \end{bmatrix},\ \mathbf{h}_3 = \begin{bmatrix} \mathbf{h}_{3,1} \\ \vdots \\ \mathbf{h}_{3,N} \end{bmatrix},\ \boldsymbol{\epsilon}_3 = \begin{bmatrix} \boldsymbol{\epsilon}_{3,1} \\ \vdots \\ \boldsymbol{\epsilon}_{3,N} \end{bmatrix},$$

$$\mathbf{G}_{3,j} = \begin{bmatrix} \vdots \\ \mathbf{g}_{ij} \\ \vdots \end{bmatrix}, \quad \mathbf{h}_{3,j} = \begin{bmatrix} \vdots \\ \hat{d}_{ij} \\ \vdots \end{bmatrix}, \quad \boldsymbol{\epsilon}_{3,j} = \begin{bmatrix} \vdots \\ \epsilon_{ij} \\ \vdots \end{bmatrix}_{i \in \mathcal{A}_j \cup \mathcal{B}_j}$$

and $\mathbf{g}_{ij} = [\mathbf{g}_{ij}^y, \ \mathbf{g}_{ij}^p]$,

$$\begin{aligned}
\mathbf{g}_{ij}^y &= \left[\mathbf{0}_{1\times 2(j-1)}, \hat{\mathbf{u}}_{ij}^T, \mathbf{0}_{1\times 2(N-j)}\right], \ i \in \mathcal{A}_j \\
\mathbf{g}_{ij}^y &= \left[\mathbf{0}_{1\times 2(j-1)}, \hat{\mathbf{u}}_{ij}^T, \mathbf{0}_{1\times 2(i-j-1)}, -\hat{\mathbf{u}}_{ij}^T, \mathbf{0}_{1\times 2(N-i)}\right], \ i \in \mathcal{B}_j \\
\mathbf{g}_{ij}^p &= \left[\mathbf{0}_{1\times (j-1)}, \hat{\xi}_{ij}, \mathbf{0}_{1\times (N-j)}\right], \ i \in \mathcal{A}_j \cup \mathcal{B}_j
\end{aligned}$$

Since as prior knowledge, we know that the unknown vector $\Delta\boldsymbol{\theta}_3$ is not too large, (44) can be solved by the Tikhonov-regularized LS formulation in which the cost function includes the weighted squared norm of $\Delta\boldsymbol{\theta}_3$ to keep it as small as possible. The Tikhonov-regularized LS solution of (44) is obtained as [44], [26, Ch. 6]

$$\Delta\hat{\boldsymbol{\theta}}_3 = \underset{\Delta\boldsymbol{\theta}_3 \in \mathbb{R}^{3N}}{\arg\min} \ \|\mathbf{G}_3\Delta\boldsymbol{\theta}_3 - \mathbf{h}_3\|^2 + \delta\|\Delta\boldsymbol{\theta}_3\|^2, \tag{45}$$

where δ is a regularization parameter controlling the trade-off between $\|\mathbf{G}_3\Delta\boldsymbol{\theta}_3 - \mathbf{h}_3\|^2$ and $\|\Delta\boldsymbol{\theta}_3\|^2$. The closed-form solution of (45) is given by [26, Ch. 6]

$$\Delta\hat{\boldsymbol{\theta}}_3 = \left(\mathbf{G}_3^T\mathbf{G}_3 + \delta\mathbf{I}_L\right)^{-1}\mathbf{G}_3^T\mathbf{h}_3. \tag{46}$$

Finally, the location of each source node is determined as

$$\tilde{\mathbf{x}}_j = \hat{\mathbf{x}}_j - \Delta\hat{\mathbf{x}}_j, \quad j \in \mathcal{S}. \tag{47}$$

APPENDIX C
COMPLEXITY ANALYSIS OF THE ALGORITHMS

The computational complexity of the considered algorithms based on the required number of flops is derived in this section. We assume that an addition, subtraction, multiplication, division, or square root operation in the real domain can be computed by one flop [45], [46]. For simplicity, we keep only the leading terms of the complexity expressions. We derive the complexity of cooperative approaches which includes non-cooperative case as a special case ($N = 1$). Note that the worst-case complexity is derived

without any attempt to optimize computations to take advantage of, e.g., the structure of matrices. The complexity of the considered algorithms is computed as a function of N, the number of source nodes, M, the number of anchor nodes, and $L = \sum_{j\in\mathcal{S}} |\mathcal{A}_j| + |\mathcal{B}_j|$, the total number of connections. Note that for a network with full connectivity, we have $L = N(M + (N-1)/2)$.

A. Maximum Likelihood

As previously mentioned, the ML estimator is nonlinear and nonconvex. Therefore, ML complexity highly depends on the solution method. In addition, the complexity of every method also depends on many parameters, e.g., the number of iterations, the initial point, or the solution accuracy. Gauss-Newton (GN) is the one of the most popular methods used in solving nonlinear optimization problems [32, Ch. 8]. GN is an iterative technique and requires initialization. Assuming a nonlinear problem with a set of m equations and n unknown variables, the asymptotic computational complexity ($m \gg n$) of the GN method in each iteration is $O(m^3)$ [47]. The number of iterations depends highly on the initial point and required accuracy. Assuming $O(k)$ iterations on average is required to solve a specific problem, the total complexity of the GN method is $O(km^3)$. For the proposed ML, we have $m = L$, and $n = 3N$. Consequently, the asymptotic complexity of the ML estimator in (12) is

$$\text{ML Complexity} \;\simeq\; O(kL^3). \tag{48}$$

B. Semidefinite Programming

Consider the general form of a semidefinite programming problem [25]

$$\begin{aligned} \underset{\mathbf{x}}{\text{minimize}} \quad & \mathbf{c}^T\mathbf{x} \\ \text{subject to} \quad & \mathbf{F}(\mathbf{x}) \succeq \mathbf{0}, \end{aligned} \tag{49}$$

where $\mathbf{x} \in \mathbb{R}^m$ and

$$\mathbf{F}(\mathbf{x}) = \mathbf{F}_0 + \sum_{i=1}^{m} x_i\mathbf{F}_i.$$

The available data includes the vector $\mathbf{c} \in \mathbb{R}^m$ and $m+1$ symmetric matrices $\mathbf{F}_0, \ldots, \mathbf{F}_m \in \mathbb{R}^{n\times n}$. An SDP problem can be solved by iterative optimization techniques, e.g., interior-point methods [25], [26]. The worst-case computational complexity of solving SDP in each iteration is $O(m^2n^2)$ [25]. The number of iterations is also bounded by $O(\sqrt{n}\log(1/\epsilon))$, where ϵ is the accuracy of SDP solution [25], [34]. For

the proposed SDP, we have $m \simeq L + 3N$ and $n \simeq N$. Therefore, the complexity of the SDP in (16) is

$$\text{SDP Complexity} \;\simeq\; O(\sqrt{N}(L+3N)^2 N^2 \log(1/\epsilon)). \tag{50}$$

C. Linear estimator

Consider a weighted linear least squares problem with a set of m equations and n unknown variables defined as [32, Ch. 5]

$$\hat{\boldsymbol{\theta}} = (\mathbf{G}^T\mathbf{W}\mathbf{G})^{-1}\mathbf{G}^T\mathbf{W}\mathbf{h}, \tag{51}$$

where $\boldsymbol{\theta} \in \mathbb{R}^n$, $\mathbf{G} \in \mathbb{R}^{m\times n}$, $\mathbf{W} \in \mathbb{R}^{m\times m}$, and $\mathbf{h} \in \mathbb{R}^m$. Computing $\hat{\boldsymbol{\theta}}$ includes five matrix multiplications and one matrix inversion. Therefore, the computational complexity of (51) is $O(2m^2n+mn^2+mn+n^3+n^2)$ [45], [48]. Assuming $m \gg 2n$, the complexity of (51) is upper bounded by $O(m^3)$. The complexity of the proposed LLS algorithms can be simply expressed as follows,

TABLE V
COMPLEXITY OF LLS ALGORITHMS.

Algorithm	m	n	Complexity
LLS in (28)	$\lvert\mathcal{A}_j\rvert$	4	$O(8\lvert\mathcal{A}_j\rvert^2 + 20\lvert\mathcal{A}_j\rvert + 80)$
LLS in (34)	4	3	$O(180)$
LLS in (46)	L	$3N$	$O(6L^2N + 9LN^2)$
PLE in (18)	L	$N+1$	$O(2L^2(N+1) + L(N+1)^2)$

The cooperative LLS algorithm includes (28), (34) which are calculated for N source nodes and (46). Therefore, from Table V, the total computational complexity of the cooperative LLS approach is

$$\text{LLS Complexity} \;\simeq\; O(6L^2N + 9LN^2 + \sum_{j\in\mathcal{S}} 8|\mathcal{A}_j|^2). \tag{52}$$

REFERENCES

[1] N. Patwari, J. N. Ash, S. Kyperountas, A. O. Hero III, R. L. Moses, and N. S. Correal, "Locating the nodes: Cooperative localization in wireless sensor networks," *IEEE Signal Process. Mag.*, vol. 22, no. 4, pp. 54–69, July 2005.

[2] N. Patwari, A. O. Hero III, M. Perkins, N. S. Correal, and R. J. O'Dea, "Relative location estimation in wireless sensor networks," *IEEE Trans. Signal Process.*, vol. 51, no. 8, pp. 2137–2148, August 2003.

[3] X. Li, "Collaborative localization with received-signal strength in wireless sensor networks," *IEEE Trans. Veh. Technol.*, vol. 56, no. 6, pp. 3807–3817, November 2007.

[4] H. C. So and L. Lin, "Linear least squares approach for accurate received signal strength based source localization," *IEEE Trans. Signal Process.*, vol. 59, no. 8, pp. 4035–4040, August 2011.

[5] I. Guvenc and C.-C. Chong, "A survey on TOA based wireless localization and NLOS mitigation techniques," *IEEE Commun. Surveys Tuts.*, vol. 11, no. 3, pp. 107–124, 2009.

[6] S. Venkatesh and R. M. Buehrer, "NLOS mitigation using linear programming in ultrawideband location-aware networks," *IEEE Trans. Veh. Technol.*, vol. 56, no. 5, pp. 3182–3198, September 2007.

[7] A. Catovic and Z. Sahinoglu, "The Cramer-Rao bounds of hybrid TOA/RSS and TDOA/RSS location estimation schemes," *IEEE Commun. Lett.*, vol. 8, no. 10, pp. 626–628, October 2004.

[8] L. Yang and K. C. Ho, "An approximately efficient TDOA localization algorithm in closed-form for locating multiple disjoint sources with erroneous sensor positions," *IEEE Trans. Signal Process.*, vol. 57, no. 12, pp. 4598–4615, December 2009.

[9] M. Sun and K. C. Ho, "An asymptotically efficient estimator for TDOA and FDOA positioning of multiple disjoint sources in the presence of sensor location uncertainties," *IEEE Trans. Signal Process.*, vol. 59, no. 7, pp. 3434–3440, July 2011.

[10] R. M. Vaghefi, M. R. Gholami, and E. G. Ström, "Bearing-only target localization with uncertainties in observer position," in *Proc. IEEE PIMRC*, September 2010, pp. 238–242.

[11] L. Cong and W. Zhuang, "Hybrid TDOA/AOA mobile user location for wideband CDMA cellular systems," *IEEE Trans. Wireless Commun.*, vol. 1, no. 3, pp. 439–447, July 2002.

[12] K. W. Cheung, H. C. So, W.-K. Ma, and Y. T. Chan, "A constrained least squares approach to mobile positioning: Algorithms and optimality," *EURASIP J. Appl. Signal Process.*, pp. 1–23, 2006.

[13] R. W. Ouyang, A. K.-S. Wong, and C.-T. Lea, "Received signal strength-based wireless localization via semidefinite programming: Noncooperative and cooperative schemes," *IEEE Trans. Veh. Technol.*, vol. 59, no. 3, pp. 1307–1318, March 2010.

[14] Y.-T. Chan, H. Y. C. Hang, and P. chung Ching, "Exact and approximate maximum likelihood localization algorithms," *IEEE Trans. Veh. Technol.*, vol. 55, no. 1, pp. 10–16, Januray 2006.

[15] X. Sheng and Y.-H. Hu, "Maximum likelihood multiple-source localization using acoustic energy measurements with wireless sensor networks," *IEEE Trans. Signal Process.*, vol. 53, no. 1, pp. 44–53, Januray 2005.

[16] C. Meng, Z. Ding, and S. Dasgupta, "A semidefinite programming approach to source localization in wireless sensor networks," *IEEE Signal Process. Lett.*, vol. 15, pp. 253–256, 2008.

[17] C. Meesookho, U. Mitra, and S. Narayanan, "On energy-based acoustic source localization for sensor networks," *IEEE Trans. Signal Process.*, vol. 56, no. 1, pp. 365–377, January 2008.

[18] M. Sun and K. C. Ho, "Successive and asymptotically efficient localization of sensor nodes in closed-form," *IEEE Trans. Signal Process.*, vol. 57, no. 11, pp. 4522–4537, November 2009.

[19] R. M. Vaghefi, M. R. Gholami, and E. G. Ström, "RSS-based sensor localization with unknown transmit power," in *Proc. IEEE ICASSP*, May 2011, pp. 2480–2483.

[20] P. Biswas, T.-C. Liang, K.-C. Toh, Y. Ye, and T.-C. Wang, "Semidefinite programming approaches for sensor network localization with noisy distance measurements," *IEEE Trans. Autom. Sci. Eng.*, vol. 3, no. 4, pp. 360–371, October 2006.

[21] A. M.-C. So and Y. Ye, "Theory of semidefinite programming for sensor network localization," *Math. Program., Series B*, vol. 109, no. 2–3, pp. 367–384, October 2007.

[22] R. M. Vaghefi and R. M. Buehrer, "Cooperative sensor localization with NLOS mitigation using semidefinite programming," in *Proc. 9th Workshop on Positioning, Navigation and Communication (WPNC)*, March 2012.

[23] G. Wang and K. Yang, "A new approach to sensor node localization using RSS measurements in wireless sensor networks," *IEEE Trans. Wireless Commun.*, vol. 10, no. 5, pp. 1389–1395, May 2011.

[24] E. Xu, Z. Ding, and S. Dasgupta, "Reduced complexity semidefinite relaxation algorithms for source localization based on time difference of arrival," *IEEE Trans. Mob. Comput.*, vol. 10, no. 9, pp. 1276–1282, September 2011.

[25] L. A. Vandenberghe and S. B. Boyd, "Semidefinite programming," *SIAM Rev.*, vol. 38, no. 1, pp. 49–95, March 1996.

[26] S. Boyd and L. Vandenberghe, *Convex Optimization*. Cambridge, UK: Cambridge University Press, 2004.

[27] S. Kim, H. Jeon, and J. Ma, "Robust localization with unknown transmission power for cognitive radio," in *Proc. IEEE MILCOM*, October 2007, pp. 1–6.

[28] J. H. Lee and R. M. Buehrer, "Location estimation using differential RSS with spatially correlated shadowing," in *Proc. IEEE GLOBECOM*, December 2009, pp. 1–6.

[29] G. Wang and K. Yang, "Efficient semidefinite relaxation for energy-based source localization in sensor networks," in *Proc. IEEE ICASSP*, 2009, pp. 2257–2260.

[30] M. R. Gholami, M. Rydström, and E. G. Ström, "Positioning of node using plane projection onto convex sets," in *Proc. IEEE WCNC*, April 2010, pp. 1–5.

[31] C. Liu, K. Wu, and T. He, "Sensor localization with ring overlapping based on comparison of received signal strength indicator," in *Proc. IEEE MASS*, October 2004, pp. 516–518.

[32] S. M. Kay, *Fundamentals of Statistical Signal Processing: Estimation Theory*. Upper Saddle River, NJ: Prentice-Hall, 1993.

[33] W. H. Foy, "Position-location solution by Taylor-series estimation," *IEEE Trans. Aerosp. Electron. Syst.*, vol. 12, no. 3, pp. 187–194, March 1976.

[34] J. F. Sturm, "Using SeDuMi 1.02, a MATLAB toolbox for optimization over symmetric cones," 1998.

[35] R. H. Tütüncü, K. C. Toh, and M. J. Todd, "Solving semidefinite-quadratic-linear programs using SDPT3," *Math. Program.*, vol. 95, no. 2, pp. 189–217, February 2003.

[36] J. Kivinen, X. Zhao, and P. Vainikainen, "Empirical characterization of wideband indoor radio channel at 5.3 GHz," *IEEE Trans. Antennas Propag.*, vol. 49, no. 8, pp. 1192–1203, August 2001.

[37] X. Li, "RSS-based location estimation with unknown pathloss model," *IEEE Trans. Wireless Commun.*, vol. 5, no. 12, pp. 3626–3633, December 2006.

[38] P. Biswas, T.-C. Lian, T.-C. Wang, and Y. Ye, "Semidefinite programming based algorithms for sensor network localization," *ACM Trans. Sen. Netw.*, vol. 2, no. 2, pp. 188–220, May 2006.

[39] M. Grant and S. Boyd, "CVX: Matlab software for disciplined convex programming, version 1.21," http://cvxr.com/cvx, May 2010.

[40] D. Torrieri, "Statistical theory of passive location systems," *IEEE Trans. Aerosp. Electron. Syst.*, vol. 20, no. 2, pp. 183–198, July 1984.

[41] T. Jia and R. M. Buehrer, "On the optimal performance of collaborative position location," *IEEE Trans. Wireless Commun.*, vol. 9, no. 1, pp. 374–383, January 2010.

[42] Y. T. Chan and K. C. Ho, "A simple and efficient estimator for hyperbolic location," *IEEE Trans. Signal Process.*, vol. 42, no. 8, pp. 1905–1915, August 1994.

[43] M. R. Gholami, S. Gezici, E. G. Ström, and M. Rydström, "Positioning algorithms for cooperative networks in the presence of an unknown turn-around time," in *Proc. IEEE SPAWC*, June 2011, pp. 166–170.

[44] ——, "Hybrid TW-TOA/TDOA positioning algorithms for cooperative wireless networks," in *Proc. IEEE ICC*, June 2011, pp. 1–5.

[45] G. Golub and C. F. V. Loan, *Matrix computations*, 3rd ed. Johns Hopkins University Press, 1996.

[46] M. R. Gholami, S. Gezici, and E. G. Ström, "Improved position estimation using hybrid TW-TOA and TDOA in cooperative networks," *IEEE Trans. Signal Process.*, vol. 60, no. 7, pp. 3770–3785, July 2012.

[47] C. A. Floudas and P. M. Pardalos, *Encyclopedia of Optimization*, 2nd ed. New York, NY: Springer-Verlag, 2009.

[48] S. Arora and B. Barak, *Computational Complexity: A Modern Approach*. Cambridge University Press, 2009.